J Pharmacol Sci **118**, 288 – 294 (2012)

Journal of Pharmacological Sciences

Full Paper

Cannabinoid Receptor Activation Disrupts the Internal Structure of Hippocampal Sharp Wave–Ripple Complexes

Yi Sun[1,2], Hiroaki Norimoto[1], Xiao-Ping Pu[2], Norio Matsuki[1], and Yuji Ikegaya[1,*]

[1]*Laboratory of Chemical Pharmacology, Graduate School of Pharmaceutical Sciences, The University of Tokyo, Tokyo 113-0033, Japan*
[2]*Department of Molecular and Cellular Pharmacology, School of Pharmaceutical Sciences, Peking University Health Science Center, Beijing 100191, China*

Received October 23, 2011; Accepted December 22, 2011

Abstract. Cannabinoid agonists impair hippocampus-dependent learning and memory. Using mouse hippocampal slice preparations, we examined the effect of anandamide, an endogenous cannabinoid, on sharp wave–ripple (SW-R) complexes, which are believed to mediate memory consolidation during slow-wave sleep or behavioral immobility. Anandamide reduced the frequency of SW-Rs recorded from the CA3 region, and this effect was abolished by AM251, a cannabinoid CB1–receptor antagonist. We further addressed the action of anandamide using a functional multineuron calcium imaging technique. Anandamide reduced the firing rate of hippocampal neurons as well as disrupted the temporal coordination of their firings during SW-R.

Keywords: hippocampus, local field potential, memory consolidation, endocannabinoid, type 1 cannabinoid (CB1) receptor

Introduction

In the central nervous system, endocannabinoids, such as anandamide (*N*-arachidonoylethanolamide, AEA) and 2-arachidonoylglycerol, are synthesized and released mainly from postsynaptic neurons. They reduce the activity of voltage-sensitive N-, P/Q-, and L-type calcium channels and facilitate G protein–activated inwardly rectifying potassium channels (1, 2). The modulations of these ion channels may contribute to suppression of depolarization-triggered neurotransmitter release (3). This action is mediated by G protein–coupled type 1 cannabinoid (CB1) receptors, which are expressed primarily in the hippocampus, neocortex, cerebellum, and basal ganglia (4, 5).

At the systems level, the cannabinoid cascade is reported to play critical roles in learning and memory. For example, systemic administrations of endocannabinoids, the natural cannabinoid agonist *Δ*9-tetrahydrocannabinol (*Δ*9-THC), or its synthetic analogues CP55940 and WIN55,212-2 impair hippocampus-dependent tasks (6). This impairment is rescued by SR141716A, a CB1-receptor antagonist (7, 8). Importantly, direct administrations of *Δ*9-THC, CP-55940, or WIN55,212-2 into the hippocampus also attenuate the learning ability, and the effects are prevented by AM281, a CB1-receptor antagonist (9 – 13), indicating that hippocampal CB1 receptors have a pivotal role in cognition. Consistent with this, cannabinoid receptor activation inhibits the induction of hippocampal synaptic plasticity, such as long-term potentiation (14, 15) and long-term depression (16), in hippocampal slices.

Hippocampus-dependent memory is formed by diverse types of network activity, among which sharp wave–ripple complexes (SW-Rs) reflect transient neuronal synchronization originating from the CA3 (or partly CA1) region. SW-Rs occur during slow-wave sleep and behavioral immobility and are believed to transfer tentative hippocampal information to more stable neocortical storage (17, 18). Consistent with this hypothesis, hippocampal neurons that fired together during exploratory behavior tend to synchronize again during SW-Rs (19, 20). Moreover, online-triggered suppression of hippocampal SW-Rs during post-training consolidation periods impairs spatial memory (21), which suggests that SW-Rs are required to stabilize once acquired recent

*Corresponding author. ikegaya@mol.f.u-tokyo.ac.jp
Published online in J-STAGE on February 1, 2012 (in advance)
doi: 10.1254/jphs.11199FP

memory. Robbe et al. (22) showed that Δ9-THC and CP-55940 attenuate the power of local field potentials (LFPs) that include SW-Rs in head-restrained or freely moving rats. The present study is thus aimed to evaluate the effect of endogenous cannabinoids on SW-Rs in an in vitro experimental model of SW-Rs (23, 24).

Materials and Methods

Animal ethics

Experiments were performed with the approval of the animal experiment ethics committee at the University of Tokyo (approval number 19-35) according to the University of Tokyo guidelines for the care and use of laboratory animals.

Chemicals

AEA, AM251, and (5*Z*,8*Z*,11*Z*,14*Z*)-*N*-(4-hydroxy-2-methylphenyl)-5,8,11,14-eicosatetraenamide (VDM-11) were purchased from Tocris Bioscience (Bristol, UK). The stock solution was prepared in anhydrous ethanol at a concentration of 14 mM, which was then diluted to the final concentration with oxygenated artificial cerebrospinal fluid (aCSF) consisting of 127 mM NaCl, 26 mM $NaHCO_3$, 3.5 mM KCl, 2.0 mM $CaCl_2$, 1.3 mM $MgSO_4$, 1.24 mM NaH_2PO_4, and 10 mM D-glucose. Drugs were continuously bath-applied after a baseline recording period of 5 min. Control groups were perfused with aCSF alone.

Slice preparations

Male C57-BL/6J mice (SLC, Shizuoka) at postnatal 3 − 5 weeks were decapitated under deep ether anesthesia. The brains were quickly isolated and immersed in the ice-cold, oxygenated aCSF for 10 min. After removal of the cerebellum, the hemisphere was glued to a vibratome chamber and pseudo-horizontally sliced at an angle of 12.7° in the front-occipital direction (25) using a vibratome (thickness: 400 μm) (LEICA VT1200S; Leica, Nussloch, Germany) in the ice-cold, oxygenated modified aCSF containing 222.1 mM sucrose, 27 mM $NaHCO_3$, 1.4 mM NaH_2PO_4, 2.5 mM KCl, 1.0 mM $CaCl_2$, 7 mM $MgSO_4$, and 0.5 mM ascorbic acid (26). The slice was transferred to a submerged chamber filled with oxygenated aCSF (pre-warmed at 37°C) and stored for more than 90 min.

Electrophysiological recording

Recordings were conducted in a submersion-type recording chamber (volume: 1.8 ml) perfused with aCSF (saturated with 95% O_2 and 5% CO_2 at 37°C) at about 10 ml/min. LFPs were recorded from the stratum pyramidale in the CA3 region using glass microelectrodes (tip diameter: 5 − 10 μm; resistance: 1 − 3 MΩ) filled with aCSF. Signals were obtained at 20 kHz using a Multiclamp 700B amplifier and pCLAMP10.2 software and low-pass filtered at 2 kHz. Recordings were started 20 min after basal LFPs became stable. Each slice was used for only one experimental treatment. Traces were reduced to 5 kHz before data processing with a custom-written MATLAB-based program (Mathworks, Natick, MA, USA). The slow and fast components in LFP fluctuations were extracted by filtering at different corner frequencies. For sharp waves, raw LFP traces were band-pass filtered between 1 and 50Hz, and sharp-wave events were detected by setting a threshold at 5 − 10 times above the standard deviation (S.D.) of the event-free baseline noise. For ripples, LFP traces were band-pass filtered between 100 and 300 Hz and thresholded at 5 × SDs of the event-free baseline noise. All detected events were scrutinized by eye and manually rejected if they were erroneously detected.

Functional multineuron calcium imaging (fMCI)

Oregon Green BAPTA-1AM (OGB1; Invitrogen, Carlsbad, CA, USA) was bolus injected into the CA1 stratum pyramidale, as described previously (27). OBG1 was dissolved in 10% Pluronic F-127/DMSO (Invitrogen) at a concentration of 2 mM. Immediately before use, the solution was 10 × diluted with aCSF and loaded into pipettes (1 – 2 MΩ). The tip of the pipette was inserted into the CA1 stratum pyramidale, and a pressure was applied using a 10-ml syringe pressurizer (50 – 60 hPa for 3 – 5 min). Fluorophores were excited at 488 nm with a laser diode (HPU50101PFS; FITEL, Tokyo) and visualized using a 507-nm long-pass emission filter. Images were collected at 50 frames/s using a 16 × objective (CFI75LWD16xW; Nikon, Tokyo), a Nipkow-disk confocal microscope (CSU-X1; Yokogawa Electric, Tokyo), and a cooled EM-CCD camera (iXon DU897; Andor, Belfast, UK) (28). The fluorescence change was measured as $(F_t - F_0) / F_0$, where the F_t is the fluorescence intensity at a given time point; F_0 is the baseline. Spike-triggered calcium signals were semi-automatically detected with a custom-written program in Visual Basic version 6.0 (Microsoft, Seattle, WA, USA) and visually inspected directly (29).

Results

SW-Rs recorded from the stratum pyramidale are characterized by transient field sources that are superimposed by fast oscillations at 120 − 250 Hz (30). We recorded spontaneous LFPs from the CA3 stratum pyramidale of naïve ventral hippocampal slices. LFPs became stable within about 30 min after the recording electrode

was placed. During this period, the amplitude and frequency of LFPs reached the maximum values and thereafter remained stable for several hours. In stable states, spontaneous large potentials continued to occur intermittently in all slices tested (Fig. 1A, top). The mean event frequency was 73 ± 17 per minute (mean ± S.D. of 33 slices from 33 mice). The fast Fourier transform (FFT) of the LFP traces revealed two distinct peaks at frequencies of 1 − 25 Hz and 200 − 250 Hz in the power spectrum, typical of SW-Rs (Fig. 1B). We extracted the frequency components by filtering LFP traces, according to the method introduced by Maier et al. (23). The band-pass filtering of 1 − 50 and 100 − 300 Hz produced sharp waves and spindle-shaped fast oscillations reminiscent of ripples, respectively (Fig. 1A, bottom). The latter oscillatory pattern consisted of 4 – 8 sinusoid waves per event (31).

We perfused slices with AEA for 20 min to examine the action of endocannabinoids on SW-Rs. We found that SW-R events gradually decreased in number during a period of a few minutes after wash-in of 1 μM AEA and reached a steady state after about 5 min (Fig. 2A). The suppression of SW-Rs reversed within about 5 min after AEA wash-out. The effect of AEA was dose-dependent (Fig. 2B); 1 μM AEA decreased the SW-R frequency from 75 ± 18 to 56 ± 16 min^{-1} ($P = 0.017$, $t_7 = 3.07$, paired t-test, n = 8 slices from 7 mice), whereas 0.5 μM AEA did not induce a significant change ($P = 0.47$, $t_4 = 0.79$, paired t-test, n = 5 slices from 5 mice). We further confirmed the dose dependency using one-way ANOVA for all three cohorts, i.e., slices treated with 0 μM (control), 0.5 μM AEA, and 1.0 μM AEA (Fig. 2C). The overall effect of AEA was significant ($P = 0.006$, $F_{2,18} = 7.04$). *Post hoc* analyses using three different statistical tests, Fisher's protected least significant difference test, Sheffe's test, and Bonferroni/Dunn test, revealed a significant difference was found between the control and 1.0 μM AEA ($P = 0.0027$, $P = 0.0098$, $P = 0.0065$, respectively), but not between the control and 0.5 μM AEA ($P = 0.48$, $P = 0.77$, $P = 0.21$, respectively).

The same experiments were repeated in the presence of 2 μM AM251, a CB1-receptor antagonist (Fig. 2D). We found that AM251 alone did not induce a significant change in the SW-R frequency ($P = 0.24$, $t_4 = 1.38$, paired t-test, n = 5 slices from 5 mice), suggesting that the endocannabinoid system is not active under resting conditions of hippocampal slices. Consistent with this idea, 10 μM VDM-11, an inhibitor of endocannabinoid uptake, also failed to change the SW-R frequency ($P = 0.98$, $t_4 = 0.03$, paired t-test, n = 5 slices from 4 mice). In slices pretreated with AM251 for 10 min, 1 μM AEA did not decrease the SW-R frequency ($P = 0.59$, $t_5 = 0.58$, paired t-test, n = 6 slices from 6 mice). Thus, AEA-induced SW-R suppression was mediated by CB1 receptors. The data for the entire group were also statistically analyzed; one-way ANOVA revealed a across-group significance ($P = 0.011$, $F_{2,15} = 6.16$) and *post hoc* analyses revealed a significance between AEA alone and AEA + AM251 ($P = 0.012$, $P = 0.038$, $P = 0.092$, respectively, for Fisher's protected least significant difference test, Sheffe's test, and Bonferroni/Dunn test), but not between AEA + AM251 and AM251 alone ($P = 0.71$, $P = 0.93$, $P = 0.22$, respectively).

To examine the spatiotemporal dynamics of neuronal activity during SW-Rs, we used an fMCI technique, which probes spikes emitted by individual neurons through action potential–evoked calcium elevations in the cell bodies (32). The calcium transients were monitored at 50 frames per second from an area of approximately 500×300 μm^2 that contained an average of 58 ± 23 neurons (mean ± S.D. of 5 slices from 5 mice,

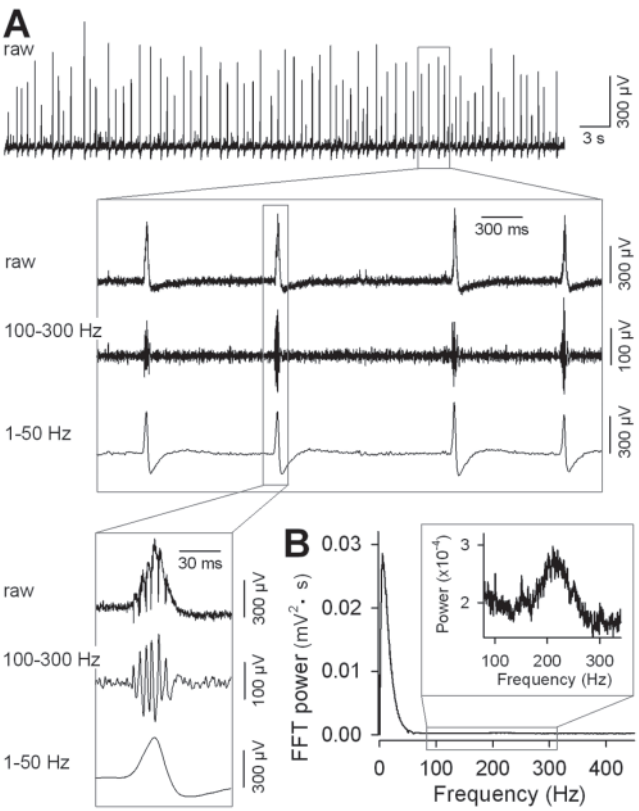

Fig. 1. Electrophysiological recording of spontaneous SW-Rs from hippocampal slices. A: Raw LFP traces recorded from the CA3 stratum pyramidale. The boxed regions were time-expanded into the middle and bottom boxes, where LFPs were filtered at band passes of 100 − 300 Hz (for extracting ripples) and 1 − 50 Hz (for extracting sharp waves). B: Power spectrum of LFPs shown in A (10 min in length) peaked at about 200 Hz.

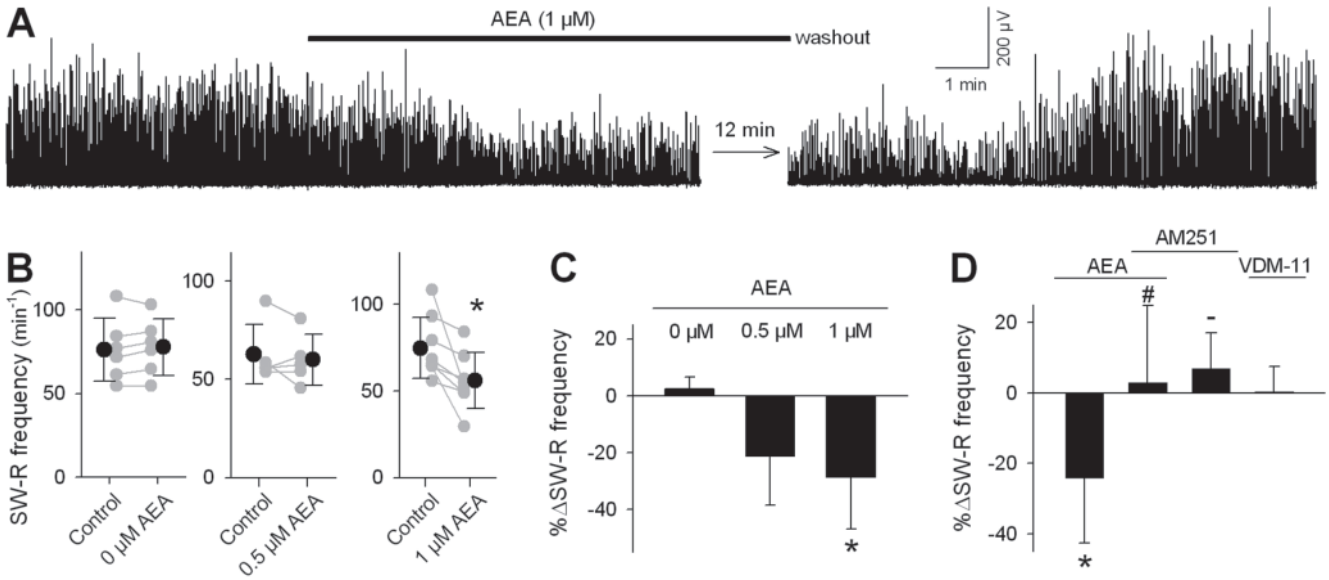

Fig. 2. AEA-induced suppression of SW-Rs. A: Representative LFP traces before, during, and after 20-min application of 1 μM AEA. B, C: Dose dependency of AEA-induced changes (B) and change ratios (C) in the SW-R frequency. *$P < 0.05$ vs. s pre-application control, paired *t*-test (B) or Fisher's protected least significant difference test, Sheffe's test, and Bonferroni/Dunn test (C). D: AEA-induced change ratio in the SW-R frequency in the absence or presence of 2 μM AM251. Neither 2 μM AM251 alone nor 10 μM VDM-11 alone affected the SW-R frequency. *$P < 0.05$ and $^{-}P > 0.1$ vs. pre-treatment control, $^{\#}P < 0.05$ vs. AEA alone; Fisher's protected least significant difference test, Sheffe's test, and Bonferroni/Dunn test. Data are means ± S.D.s.

ranging from 38 to 96 neurons). In the same area, LFPs was simultaneously recorded (Fig. 3A). Representative data are shown in Fig. 3B, indicating that the activity frequency varied from neuron to neuron and that some of the activities were time-locked to SW-R events. For the entire datasets, 55.7% ± 25.0% of the total activities (mean ± S.D of 5 slices) occurred from –50 ms to 50 ms after the peak timings of sharp waves, and the remaining 44.3% ± 25.0% occurred independently of SW-Rs. The mean activity rates reached the maximum at the peak timings of sharp waves, and the half-peak width of the rate increase was 80 ms (Fig. 3C). Neuronal activities during individual SW-R events were rather sparse; on average, only 1.7% ± 1.1% of the neurons were activated during each SW-R (mean ± S.D. of 188 SW-R events), whereas 62.7% of the total 292 neurons participated in at least one SW-R event during our observation periods.

We compared the activity patterns before and during bath application of 1 μM AEA. Representative data in Fig. 3B suggest not only that AEA decreased the overall activity level but also that a different set of the neurons became participants in SW-Rs in the presence of AEA. We thus quantified the internal activity structures of SW-Rs. In the presence of AEA, SW-Rs still accompanied time-locked activation of neuronal activities, but the number of neurons activated during individual SW-Rs was reduced (Fig. 3C). AEA reduced the overall frequency of activities (Fig. 3D; $P = 0.0009$, $t_{291} = 3.36$, paired *t*-test). This reduction was likely to attribute to a decrease in SW-R-locked activity (Fig. 3D; $P < 0.0001$., $t_{291} = 8.19$, paired *t*-test) because AEA did not affect the frequency of SW-R-irrelevant activity (Fig. 3D; $P = 0.077$, $t_{291} = 1.77$, paired *t*-test). To address the activity pattern, we plotted the activity frequency of individual neurons in the space of 'before' *versus* 'during' AEA application (Fig. 3: E, F). We failed to find a correlation between the overall activity levels before and during AEA application (Fig. 3E left, $R^2 = 0.076$, n = 292 neurons). The lack of a correlation held true when SW-R-locked activity alone was considered (Fig. 3E right, $R^2 = 0.112$, n = 292 neurons). Therefore, AEA altered the network state, which is defined as a set of instantaneously active neurons.

Discussion

We discovered that in acute hippocampal slices, AEA, an endocannabinoid, reduced the frequency of SW-Rs in a dose-dependent manner through CB1-receptor activation and that this effect was accompanied by a change in the internal structure of neuronal network activity. Pioneer studies reported that CB1-receptor activation results in a decrease in the power of SW-R–relevant oscillations in vivo (22) and in vitro (33, 34); however, no studies

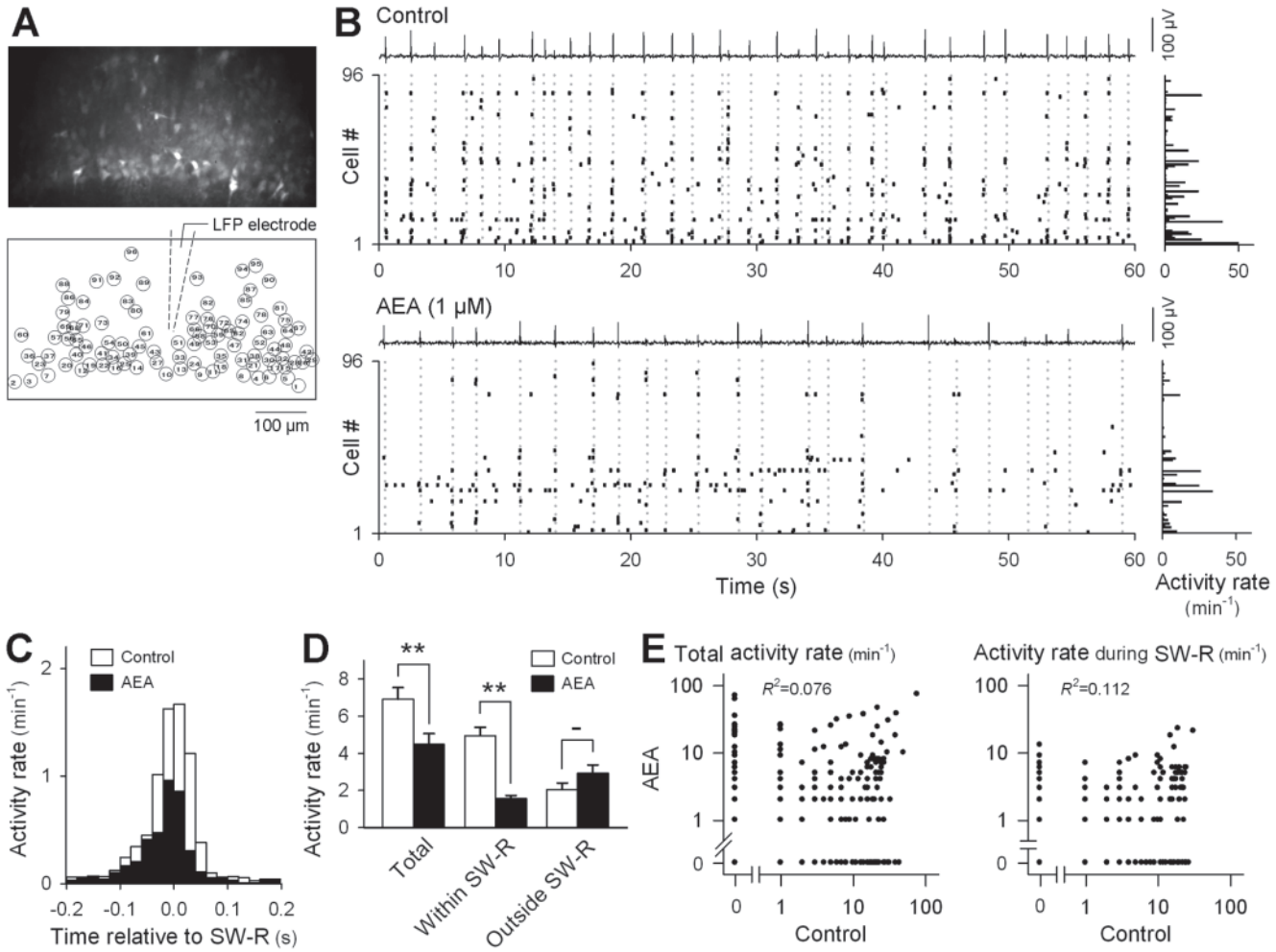

Fig. 3. AEA-induced reorganization of spiking patterns during SW-Rs. A: Typical confocal image (top) and cell map (bottom) of 96 neurons monitored from the CA1 stratum pyramidale in a OGB-1–loaded slice (top). B: Spiking patterns of the 96 neurons shown in A before and during bath application of 1 μM AEA. Dots in the raster plots indicate the onset timings of spike-evoked somatic calcium transients. Simultaneously recorded LFPs are shown above each raster plot. Gray broken lines indicate the timings of SW-R events. Right histograms indicate the activity frequencies of individual neurons. Movies were taken at 50 frames per second. C: SW-R–triggered average of calcium events before (white) and during (black) AEA application. n = 292 neurons of 5 slices. D: Mean activity frequencies before (white) and during (black) AEA application were measured for the entire recording sessions (left), during SW-R events (middle), and for the periods in the absence of SW-R (right). $^{**}P < 0.01$; paired *t*-test, n = 5 slices. Data are means ± S.D.s. E: The frequencies for the total activities (left) and activities during SW-R events (right) are plotted in a space of before vs. during AEA application. Each dot indicates data of a single neuron. n = 292 neurons.

have addressed how it disturbs the internal structure of SW-Rs. Therefore, it is intriguing to find that AEA did not only reduce the number of neurons that participated in SW-Rs but also altered the subsets of active neurons. We speculate that the disruption of the SW-R structure underlies cannabinoid-induced memory impairment.

Sharp waves are generally believed to reflect excitatory currents arising from neuronal activity in the CA3 region of the hippocampus (35), in which pyramidal cells receive external excitatory inputs from the dentate gyrus as well as recurrent excitatory inputs from themselves. SW-Rs are complex network oscillations that apparently require the balanced contribution of glutamatergic excitation and GABAergic inhibition (25, 36, 37). Thus, cannabinoid-induced SW-R suppression may depend on modulations of the release of both glutamate and GABA.

In the hippocampus, the CA2/3 region exhibits higher CB1-receptor immunoreactivity than the CA1 region (38). In hippocampal pyramidal cells, CB1 receptors are present at presynaptic terminals of excitatory synapses (39, 40), whereas diacylglycerol lipase α, one of the enzymes that mediate endocannabinoid syntheses, is present mainly in postsynaptic spines (40). Thus, endo-

cannabinoids work as a retrograde messenger from postsynaptic to presynaptic neurons. Activation of presynaptic CB1 receptors exerts variable effects, including inhibition of voltage-gated calcium channels (2, 41, 42) and activation of inwardly rectifying potassium channels (1). As a result, it reduces transmitter release from glutamatergic terminals, resulting in a decrease in the amplitude of excitatory postsynaptic currents evoked by stimulation of presynaptic neurons. This induces short-term and long-term modulations of synaptic transmission. Activation of CB1 receptors decreases the power of kainate-induced gamma oscillations in hippocampal slices and of the theta and ripple oscillations in the in vivo hippocampus (22, 43, 44). The decreased transmitter release of pyramidal cells may reduce their excitability of pyramidal cell networks and consequently an excitatory drive of interneurons. SW-Rs are initiated, at least in part, by pyramidal excitation (23, 45) or triggered by basal glutamate release (46). Therefore, it seems plausible that AEA-induced reduction of glutamate release is responsible for AEA-induced SW-R suppression.

CB1 receptors are also expressed on the axon terminals of GABAergic interneurons (5), particularly in the axons of CA3 basket cells (47, 48). An essential task of these interneurons is to prevent neuronal overexcitation and to avoid the development of pathological states of the network activity, but they have more complex roles, rather than generalized inhibition, which includes phasic inhibition that generates or regulates rhythmic activities in neuronal networks (49). A notable example is basket cells that generate and maintain hippocampal theta and gamma oscillations by phasing and synchronizing the activity of a large population of pyramidal cells. Recent observations show that $GABA_A$-receptor antagonists disrupt SW-Rs (37), an effect that is similar to the AEA-inhibited SW-R suppression observed in the present study. Thus, AEA-reduced release of both glutamate and GABA may cause disorganization of the network activity and thereby disrupt SW-Rs.

Acknowledgments

We are grateful to Mika Mizunuma for her technical advice and support. This work was supported in part by the Funding Program for Next Generation World-Leading Researchers (no. LS023) and Grants-In-Aid from the State Scholarship Fund managed under China Scholarship Council.

References

1 Guo J, Ikeda SR. Endocannabinoids modulate N-type calcium channels and G-protein-coupled inwardly rectifying potassium channels via CB1 cannabinoid receptors heterologously expressed in mammalian neurons. Mol Pharmacol. 2004;65:665–674.
2 Twitchell W, Brown S, Mackie K. Cannabinoids inhibit N- and P/Q-type calcium channels in cultured rat hippocampal neurons. J Neurophysiol. 1997;78:43–50.
3 Wilson RI, Nicoll RA. Endocannabinoid signaling in the brain. Science. 2002;296:678–682.
4 Ameri A. The effects of cannabinoids on the brain. Prog Neurobiol. 1999;58:315–348.
5 Freund TF, Katona I, Piomelli D. Role of endogenous cannabinoids in synaptic signaling. Physiol Rev. 2003;83:1017–1066.
6 Davies SN, Pertwee RG, Riedel G. Functions of cannabinoid receptors in the hippocampus. Neuropharmacology. 2002;42:993–1007.
7 Da S, Takahashi RN. SR 141716A prevents delta 9-tetrahydrocannabinol-induced spatial learning deficit in a Morris-type water maze in mice. Prog Neuropsychopharmacol Biol Psychiatry. 2002;26:321–325.
8 Lichtman AH, Martin BR. Delta 9-tetrahydrocannabinol impairs spatial memory through a cannabinoid receptor mechanism. Psychopharmacology (Berl). 1996;126:125–131.
9 Abush H, Akirav I. Cannabinoids modulate hippocampal memory and plasticity. Hippocampus. 2010;20:1126–1138.
10 Lichtman AH, Dimen KR, Martin BR. Systemic or intrahippocampal cannabinoid administration impairs spatial memory in rats. Psychopharmacology (Berl). 1995;119:282–290.
11 Mishima K, Egashira N, Hirosawa N, Fujii M, Matsumoto Y, Iwasaki K, et al. Characteristics of learning and memory impairment induced by delta9-tetrahydrocannabinol in rats. Jpn J Pharmacol. 2001;87:297–308.
12 Suenaga T, Kaku M, Ichitani Y. Effects of intrahippocampal cannabinoid receptor agonist and antagonist on radial maze and T-maze delayed alternation performance in rats. Pharmacol Biochem Behav. 2008;91:91–96.
13 Wegener N, Kuhnert S, Thuns A, Roese R, Koch M. Effects of acute systemic and intra-cerebral stimulation of cannabinoid receptors on sensorimotor gating, locomotion and spatial memory in rats. Psychopharmacology (Berl). 2008;198:375–385.
14 Collins DR, Pertwee RG, Davies SN. The action of synthetic cannabinoids on the induction of long-term potentiation in the rat hippocampal slice. Eur J Pharmacol. 1994;259:R7–R8.
15 Terranova JP, Michaud JC, Le Fur G, Soubrie P. Inhibition of long-term potentiation in rat hippocampal slices by anandamide and WIN55212-2: reversal by SR141716 A, a selective antagonist of CB1 cannabinoid receptors. Naunyn Schmiedebergs Arch Pharmacol. 1995;352:576–579.
16 Misner DL, Sullivan JM. Mechanism of cannabinoid effects on long-term potentiation and depression in hippocampal CA1 neurons. J Neurosci. 1999;19:6795–6805.
17 Buzsaki G. The hippocampo-neocortical dialogue. Cereb Cortex. 1996;6:81–92.
18 Kudrimoti HS, Barnes CA, McNaughton BL. Reactivation of hippocampal cell assemblies: effects of behavioral state, experience, and EEG dynamics. J Neurosci. 1999;19:4090–4101.
19 Pavlides C, Winson J. Influences of hippocampal place cell firing in the awake state on the activity of these cells during subsequent sleep episodes. J Neurosci. 1989;9:2907–2918.
20 Wilson MA, McNaughton BL. Reactivation of hippocampal ensemble memories during sleep. Science. 1994;265:676–679.
21 Girardeau G, Benchenane K, Wiener SI, Buzsaki G, Zugaro MB. Selective suppression of hippocampal ripples impairs spatial

memory. Nat Neurosci. 2009;12:1222–1223.
22 Robbe D, Montgomery SM, Thome A, Rueda-Orozco PE, McNaughton BL, Buzsaki G. Cannabinoids reveal importance of spike timing coordination in hippocampal function. Nat Neurosci. 2006;9:1526–1533.
23 Maier N, Nimmrich V, Draguhn A. Cellular and network mechanisms underlying spontaneous sharp wave-ripple complexes in mouse hippocampal slices. J Physiol. 2003;550:873–887.
24 Maier N, Morris G, Johenning FW, Schmitz D. An approach for reliably investigating hippocampal sharp wave-ripples in vitro. Plos One. 2009;4:e6925.
25 Behrens CJ, van den Boom LP, de Hoz L, Friedman A, Heinemann U. Induction of sharp wave-ripple complexes in vitro and reorganization of hippocampal networks. Nat Neurosci. 2005;8: 1560–1567.
26 Ueno S, Tsukamoto M, Hirano T, Kikuchi K, Yamada MK, Nishiyama N, et al. Mossy fiber Zn2+ spillover modulates heterosynaptic N-methyl-D-aspartate receptor activity in hippocampal CA3 circuits. J Cell Biol. 2002;158:215–220.
27 Sasaki T, Matsuki N, Ikegaya Y. Action-potential modulation during axonal conduction. Science. 2011;331:599–601.
28 Takahashi N, Sasaki T, Matsumoto W, Matsuki N, Ikegaya Y. Circuit topology for synchronizing neurons in spontaneously active networks. Proc Natl Acad Sci U S A. 2010;107:10244–10249.
29 Ikegaya Y, Aaron G, Cossart R, Aronov D, Lampl I, Ferster D, et al. Synfire chains and cortical songs: temporal modules of cortical activity. Science. 2004;304:559–564.
30 Buzsaki G, Draguhn A. Neuronal oscillations in cortical networks. Science. 2004;304:1926–1929.
31 Buzsaki G, Horvath Z, Urioste R, Hetke J, Wise K. High-frequency network oscillation in the hippocampus. Science. 1992; 256:1025–1027.
32 Takahashi N, Sasaki T, Usami A, Matsuki N, Ikegaya Y. Watching neuronal circuit dynamics through functional multineuron calcium imaging (fMCI). Neurosci Res. 2007;58:219–225.
33 Holderith N, Nemeth B, Papp OI, Veres JM, Nagy GA, Hajos N. Cannabinoids attenuate hippocampal gamma oscillations by suppressing excitatory synaptic input onto CA3 pyramidal neurons and fast spiking basket cells. J Physiol. 2011;589:4921–4934.
34 Maier N, Morris G, Schuchmann S, Korotkova T, Ponomarenko A, Böhm C, et al. Cannabinoids disrupt hippocampal sharp wave-ripples via inhibition of glutamate release. Hippocampus. In press.
35 Buzsaki G. Hippocampal sharp waves: their origin and significance. Brain Res. 1986;398:242–252.
36 Papatheodoropoulos C, Kostopoulos G. Spontaneous GABA(A)-dependent synchronous periodic activity in adult rat ventral hippocampal slices. Neurosci Lett. 2002;319:17–20.
37 Papatheodoropoulos C. Patterned activation of hippocampal network (approximately 10 Hz) during in vitro sharp wave-ripples. Neuroscience. 2010;168:429–442.
38 Bojnik E, Turunc E, Armagan G, Kanit L, Benyhe S, Yalçin A, et al. Changes in the cannabinoid (CB1) receptor expression level and G-protein activation in kainic acid induced seizures. Epilepsy Res. In press.
39 Kawamura Y, Fukaya M, Maejima T, Yoshida T, Miura E, Watanabe M, et al. The CB1 cannabinoid receptor is the major cannabinoid receptor at excitatory presynaptic sites in the hippocampus and cerebellum. J Neurosci. 2006;26:2991–3001.
40 Katona I, Urban GM, Wallace M, Ledent C, Jung KM, Piomelli D, et al. Molecular composition of the endocannabinoid system at glutamatergic synapses. J Neurosci. 2006;26:5628–5637.
41 Wilson RI, Kunos G, Nicoll RA. Presynaptic specificity of endocannabinoid signaling in the hippocampus. Neuron. 2001;31: 453–462.
42 Brown SP, Safo PK, Regehr WG. Endocannabinoids inhibit transmission at granule cell to Purkinje cell synapses by modulating three types of presynaptic calcium channels. J Neurosci. 2004;24:5623–5631.
43 Hajos N, Katona I, Naiem SS, MacKie K, Ledent C, Mody I, et al. Cannabinoids inhibit hippocampal GABAergic transmission and network oscillations. Eur J Neurosci. 2000;12:3239–3249.
44 Hajos M, Hoffmann WE, Kocsis B. Activation of cannabinoid-1 receptors disrupts sensory gating and neuronal oscillation: relevance to schizophrenia. Biol Psychiatry. 2008;63:1075–1083.
45 Papatheodoropoulos C. A possible role of ectopic action potentials in the in vitro hippocampal sharp wave-ripple complexes. Neuroscience. 2008;157:495–501.
46 Rex CS, Colgin LL, Jia Y, Casale M, Yanagihara TK, Debenedetti M, et al. Origins of an intrinsic hippocampal EEG pattern. Plos One. 2009;4:e7761.
47 Matyas F, Freund TF, Gulyas AI. Immunocytochemically defined interneuron populations in the hippocampus of mouse strains used in transgenic technology. Hippocampus. 2004;14:460–481.
48 Pitler TA, Alger BE. Postsynaptic spike firing reduces synaptic GABAA responses in hippocampal pyramidal cells. J Neurosci. 1992;12:4122–4132.
49 Farrant M, Nusser Z. Variations on an inhibitory theme: phasic and tonic activation of GABA(A) receptors. Nat Rev Neurosci. 2005;6:215–229.